Changes of Network Structure and Water Distribution in Sludge With the Stratified Extraction of Extracellular Polymeric Substances

Feng Lin
South China University of Technology
Bingyun Li (byli@scut.edu.cn)
South China University of Technology

Research Article

Keywords: Extracellular polymeric substance, Viscoelastic acoustic response, Sludge floc structure, Water distribution, Sludge dewaterability

Posted Date: October 22nd, 2021

DOI: https://doi.org/10.21203/rs.3.rs-937081/v1

Version of Record: A version of this preprint was published at Environmental Science and Pollution Research on February 23rd, 2022. See the published version at https://doi.org/10.1007/s11356-022-19075-4.

Abstract

For illustrating how extracellular polymeric substance (EPS) affected sludge water distribution, the present work comprehensively analyzed change of viscoelasticity and sludge network structure before/after EPS extraction, together with the sludge dewaterability and water distribution after biological, chemical and physical method conditioning. The results suggested the proportion of capillary water and adsorption water carried in soluble EPS (S-EPS) was 59.17% and 40.83%, and that in tightly-bound EPS (TB-EPS) was 54.77% and 45.23%, respectively. By contrast, the capillary water in loosely-bound EPS (LB-EPS) accounted for as high as 99.99%. Relative to raw sludge, adsorption water proportion in TB-EPS and S-EPS was reduced after lysozyme (LZM) or freezing-thaw conditioning, which was ascribed to reduction of EPS viscosity and the weakness of water adsorption capacity. Additionally, the sludge yield stress (τ_y) value first reduced and then increased with the extraction of EPS, and the consistency coefficient (k) also decreased from 4.23 $Pa{\cdot}s^n$ to 0.006 $Pa{\cdot}s^n$ and then slightly increased after LZM conditioning. This observation indicated the sludge system became sensitive to shearing, and its network structural strength as well as colloid elasticity first weakened and then slightly strengthened. What's more, after LZM or freezing-thaw conditioning, the sludge particle size significantly increased after TB-EPS extraction, while the sludge particle more easily absorbed water molecules, leading to the increase of the capillary water and adsorption water in sludge flocs. These changes reasonably explained the reason that sludge filtration performance was deteriorated after TB-EPS extraction.

1. Introduction

Activated sludge process is widely adopted to treat wastewater, and it results in increased amount of sludge. Generally speaking, sludge can be used in forestry building and landscaping and as the brickmaking and biogas producing material (Xiao et al., 2020). However, the great water content of sludge (95–99%) resulted in the high cost issues during transport (Masihi and Gholikandi, 2018). In this regard, sludge dewatering (i.e., sludge reduction) is the necessary treatment to reduce cost in sewage treatment plants (Zhang et al., 2019).

Actually, sludge is the heterogeneous colloidal system consisting of heavy metals, refractory organics, and microorganisms, which generate the stable suspension within water, so it is of great difficulty to separate solids from liquids (Mahmoud et al., 2011). Extracellular polymeric substance (EPS) produced the viscous force for forming a three-dimensional, gel-like, floc matrix with great hydration and charges, so as to embed microorganisms within flocs and to maintain structural integrity of sludge floc (Sakohara et al., 2007). The water could be embedded in the network structure composed of EPS (Liu et al., 2013), giving rise to diverse water types within the sludge. According to a previous study, the water in sludge is divided as four types, including free water that exists within sludge particle gap, capillary water because of tiny hole surface tension within the sludge, adsorption water that is attached onto sludge particle surface, and bound water that is trapped within the sludge microbial cells (Vaxelaire and Cezac, 2004; Chen et al., 2016). Therefore, water removal efficiency is closely associated with water types and their distributions within sludge (Chen et al., 2016). For instance, it is easy to remove free water from sludge,

but it is not easy to remove adsorption water, capillary water, or internal bound water since they have potent interaction forces with sludge matrix (Niu et al., 2013; Lin et al., 2020). Therefore, the difficulty of sludge dewatering was closely related to the adsorption water, capillary water, as well as internal bound water in the sludge.

Conventional coagulant and flocculation agents contribute to the aggregation of large flocs by fine sludge colloids by means of bridging and electrical neutralization, which would transform the capillary water and adsorption water into free water (Sakohara et al., 2007). However, the organic conditioners always have important functions in dewatering rate, yet they do not greatly affect EPS structural destruction and the internal bound water release (Lin et al., 2019). This is possibly related to the nearly constant dewatering extent after chemical conditioning. Our previous study found that lysozyme (LZM) had great potential in the dewatering of activated sludge (Lin et al., 2020). To be specific, it could destruct cell wall and EPS structure to release the capillary water, adsorption water, and internal bound water. Additionally, freezing-thaw as a physical conditioning method could destroy EPS structure and convert internal water to free water, thereby improving sludge dewatering performance (Carrasco and Gao, 2019). In consequence, both EPS and the water held within the EPS structure were thought as a critical factor affecting sludge dewatering.

Apart from that, it was found that the EPS is featured with multilayered structure including the soluble EPS (S-EPS), loosely bound EPS (LB-EPS) and tightly bound EPS (TB-EPS). Components and groups contained in S-EPS, LB-EPS and TB-EPS were different, thus leading to the diverse effect concerning each layer of EPS on the dewatering performance of sludge (Wang et al., 2017; Xiao et al., 2016). He et al. (2015) found the higher organic content in S-EPS or the lower organic content in LB-EPS could enhance the sludge dewaterability after Fenton's conditioning. Li et al. (2016) discovered the tryptophan and aromatic protein within TB-EPS and LB-EPS showed more significant effect on sludge dewaterability. Moreover, sludge rheological property was affected by EPS to a great extent. Among them, TB-EPS has gelatinizing ability, which could lead to the higher storage modulus of sludge after LB-EPS extraction (You et al., 2017). Liu et al. (2016) further pointed out that EPS structural destruction was able to reduce the yield stress and apparent viscosity of sludge, thus releasing bound water and improving sludge dewaterability. However, most research focused on the impact of EPS and sludge floc structure on its dewatering performance, which neglected the distribution of water and its impact on sludge dewatering performance.

Headspace gas chromatography (HS-GC) is an effective technique for analyzing volatile species in liquid samples that have complicated matrices (Zhang et al., 2016). A distinguishing advantage of HS-GC is that it can perform an in-situ measurement at a precisely controlled temperature (Suzuki et al., 1970). In a previous study (Lin et al., 2020), we proposed a new method for the determination of different types of water and its distribution in sludge based on a multiple headspace extraction (MHE) GC technique. This method could become a valuable tool in the quantitative analysis of water distribution in sludge, aiming at providing a good reference in the sludge dewatering related research and applications.

For clarifying the effect of EPS on water distribution, this study adopted chemical, physical, and biological conditioning approaches to change properties and structure of EPS in this paper. Then the existence form of water in sludge flocs and EPS was investigated to examine the variations of internal structure and moisture distribution in activated sludge were investigated by MHE-GC before/after S-EPS, LB-EPS and TB-EPS extraction. What's more, the effect of the EPS viscoelasticity and the structural characteristics of sludge flocs on water distribution was revealed,and thus providing the effective method for sludge dewatering research.

2. Materials And Methods

2.1 Materials

Municipal sludge (97.5%) was provided by secondary sedimentation tank of the municipal wastewater treatment plant in Guangzhou, China, and preserved under 4°C. The supplementary materials (Table S1) lists sludge major features.

2.2 Methods

2.2.1 Extraction of EPS

The S-EPS, LB-EPS, and TB-EPS were isolated from sludge via various procedures, such as centrifugation, thermal extraction and ultrasonic treatment (Guo et al., 2014). The detailed steps could be seen in the supplementary materials (Text S1).

2.2.2 Analysis of EPS

Protein concentration (PN) within the EPS was determined according to Coomassie brilliant blue approach, and bovine serum albumin (BSA) was used to be the standard (Bradford, 1976). Also, polysaccharide (PS) concentration was measured by anthrone approach, and glucose was used to be the standard (Raunkjær et al., 1994).

2.2.3 The determination of water distribution

Before and after EPS extraction, approximately 0.05 g sludge samples were collected and added into the 20 mL empty headspace vial, which was sealed at once and left for on the bench at 60 min prior to MHE-GC test. Afterwards, we put the vial into headspace sampler for automatic MHE-GC measurement. Then, water signal (i.e., peak area) during every headspace extraction process was measured using GC system.

2.2.4 Viscoelastic acoustic response analysis

Before experiments, we first injected deionized water in QCM-D for obtaining the baseline sample, until the frequency drift was lower than 0.3 Hz. Then, we injected solutions into QCM-D system in sequence (order, deionized water, background solution (0.5 wt. % NaCl solution), EPS solution, background solution (0.5 wt. % NaCl solution) and deionized water), for the purpose of obtaining the EPS viscoelastic

properties. Following every measurement, the flow lines were washed with 2% (w/w) sodium lauryl sulfate (SDS) solutions (10–15 mL) and pure water (50 mL) at a 1.5 mL/min flow rate. At last, flow chambers were dried with pure N_2 gas and the Voigt model was utilized to determine EPS viscoelastic properties.

2.2.5 Zeta potential measurement

The S-EPS, LB-EPS, and TB-EPS were isolated from sludge as shown in Sect. 2.2.1. Then, a laser diffraction instrument (Zetasizer Nano-ZS90, Malvern, UK) was adopted to measure the zeta potential of EPS.

2.2.6 Rheological tests

The rotational ARES-G2 rheometer (TA instruments, USA) was adopted for rheological tests. Peltier temperature control system was used to control the experimental temperature of 25℃, the plate diameter was set to 40 mm, and the plate spacing was set to 0.5 mm. Shear rate showed logarithmic increases from 0.01 to 1000 s^{-1} during steady shear test, for obtaining sludge viscoelasticity. Rheological data were fitted using the Herschel-Bulkley model good for depicting sludge rheology.

In dynamic measurement, the strain showed logarithmic changes between 0.01 % and 100 % for obtaining sludge structural properties and determining linear viscoelastic region (LVE). The frequency sweep was carried out under following conditions, strain, 0.1%; temperature, 25℃; frequency extent, 0.1–50 rad/s. Besides, the time sweep test between 1 and 300 s was carried out with LVE regime under 25℃ and 0.1% stain conditions.

2.2.7 Sludge floc structure analysis

The sludge particle diameter was analyzed by particle size analyzer (MS3000, Malvern, UK). The fractal dimension was measured according to Text S2 (Chakraborti et al., 2003).

2.2.8 Sludge dewaterability analysis

The sludge after S-EPS, LB-EPS, and TB-EPS extraction was re-suspended into the solution buffer, and the suspended sludge water content was 97.5%, which was the same as that of raw sludge. Then, capillary suction time (CST) instrument (Model 304M, Triton Electronics Ltd, Dunmow, UK) was employed for CST measurement.

3. Results And Discussion

3.1 Effect of EPS on the water distribution in sludge

3.1.1 Water distribution in the sludge floc structure

As observed from Table 1, the proportion of free water, capillary water, adsorption water and bound water in the raw sludge was 68.40%, 19.10%, 10% and 2.49%, respectively. After S-EPS, LB-EPS and TB-EPS

extraction, the sludge water content was decreased, the free water in sludge floc structure was gradually removed, and the proportion of capillary water, adsorption water and bound water was increased. Following TB-EPS extraction, proportion of those above-mentioned water was 17.60%, 56.15%, 15.26% and 10.99%, respectively. Compared with the raw sludge, free water proportion within sludge elevated to 70.98% after LZM conditioning, while that of bound water was slightly reduced to 1.12%. This was mainly because LZM promoted the hydrolysis of mucopolysaccharides in microbial cell wall, thus causing the release of intracellular water (Lin et al., 2019). Alterations in free water, capillary water and adsorption water within freezing-conditioned sludge were similar to that in LZM-conditioned sludge, and the proportion of bound water was gradually decreased with EPS extraction. This was owing to the transformation of bound water into the other forms water after freezing-thaw conditioning.

Table 1 Water distribution within sludge floc structure

	Water content, %			
Sample	Free water	Capillary water	Adsorption water	Bound water
RS	68.40	19.10	10.00	2.49
RS-S	44.87	43.32	9.16	2.65
RS-LB	31.17	49.48	15.52	3.83
RS-TB	17.6	56.16	15.25	10.99
LZM	70.98	18.93	8.97	1.2
LZM-S	52.45	37.98	8.29	1.28
LZM-LB	24.46	59.84	13.87	1.83
LZM-TB	18.10	64.46	15.56	1.89
FT	78.65	12.48	7.36	1.51
FT-S	51.97	36.88	9.86	1.29
FT-LB	25.23	62.02	11.64	1.11
FT-TB	16.22	70.93	12.28	0.57

Maximum  Minimum

*RS-S, RS-LB and RS-TB represent the raw sludge after S-EPS, LB-EPS and TB-EPS extraction, respectively. LZM-S, LZM-LB and LZM-TB represent the LZM conditioned sludge after the above three extraction, respectively. FT-S, FT-LB and FT-TB represent the freezing-thaw conditioned sludge after the above three extraction, respectively.

3.1.2 Quantitative analysis of water in EPS

As mentioned above, the extraction of S-EPS, LB-EPS and TB-EPS had significant effect on the water distribution in sludge floc structure. Therefore, the water in each layer of EPS was investigated in this section, so as to further illustrate the effect of EPS on the sludge water distribution.

According to the previous study, the free water exists within sludge particle gap, bound water is trapped within the sludge microbial cells, and only capillary water and adsorbed water exist in the sludge flocs network structure (Vaxelaire and Cezac, 2004; Chen et al., 2016). Therefore, the water combined by EPS includes capillary water and adsorbed water. As shown in Fig.1, the proportion of capillary water and adsorption water carried in S-EPS was 59.17% and 40.83%, respectively. And the proportion of capillary water and adsorption water contained in TB-EPS was 54.77% and 45.23%, which was similar to that in S-EPS. Different from the above, capillary water was accounted for as high as 99.99% in LB-EPS. The reason of this phenomenon was LB-EPS possessed the loose and porous structure, which could be bound with the water through the capillary adsorption (Poxon and Darby, 1997; Wang et al., 2017).

Relative to raw sludge, capillary water proportions within TB-EPS and S-EPS increased at 4.8×10^6U/g DS LZM, while that of adsorption water was decreased. In this case, LZM attacked and destroyed microbial cell wall, and organic substances and water were generated at great quantities, leading to the reduction of adsorption water in TB-EPS and S-EPS. By contrast, the water variation trend within LB-EPS was opposite to that in TB-EPS and S-EPS, where adsorption water and capillary water accounted for 25.67% and 74.33%, respectively. Moreover, adsorption water and capillary water proportions within LB-EPS were 17.16% and 82.84% at the freezing time of 5 h, respectively. This phenomenon was associated with the release of the water and organic substances in EPS and cell during the freezing process, thus resulting in the increase of the hydrophilic functional groups in LB-EPS and easy adsorption of water molecules (Carrasco and Gao, 2019).

3.2 Effect of EPS properties on water distribution

As discussed above, the variation of EPS property contributed to changing the water distribution in sludge. Therefore, this section examined the interaction between EPS and water from the perspectives of EPS viscoelasticity and charge distribution, so as to further explicit the change of water distribution in the sludge.

3.2.1 The change of EPS viscoelasticity

The higher frequency shift (Δf) and dissipation factor (ΔD) of EPS indicated the thicker adsorption layer formed on sensor crystals, mainly related to EPS viscosity and anti-shear ability (Wu et al., 2018). Consequently, the changes in EPS dissipation factor and frequency at adsorption stage could evaluate the viscoelasticity of EPS. According to Fig. S1, EPS viscosity in raw sludge was greater than that after conditioning, suggesting EPS in raw sludge could more easily adsorb water molecules. Among them, the viscosity of TB-EPS was the greatest, resulting in the higher proportion of adsorption water in TB-EPS. By contrast, with the increase of LZM dosage, the viscosity of each layer of EPS was significantly decreased. This was mostly related to the destruction of EPS structure and cell wall, leading to the reduction of EPS

shear resistance. As a result, EPS had a poor ability to resist the deformation induced by external disturbance and exhibited strong fluidity rather than elasticity (Wu et al., 2018; Lin et al., 2020). This was the reason why the proportion of adsorption water within TB-EPS and S-EPS was decreased following conditioning. Similar to the change of EPS after LZM conditioning, the viscosity of EPS also dramatically decreased after freezing-thaw conditioning in Fig. S2, which was mainly relevant to the destruction of sludge floc network structure during the freezing process.

3.2.2 The change of zeta potential

EPS had negative charges due to the numerous anionic functional groups, such as phosphate, hydroxyl, and carboxyl groups; as a result, sludge particles were charged with negative charges (Mahmoud et al., 2011; Lin et al., 2020). According to Fig. 2, zeta potential of S-EPS, LB-EPS and TB-EPS of the raw sludge was -19 mV, -15.30 mV and -14.93 mV, respectively. After LZM conditioning, the zeta potential value gradually approached to 0. This might be because the released PN possessed positively charged amino groups, which decreased negative charges on S-EPS, LB-EPS and TB-EPS in enzyme-conditioned sludge. When the LZM dosage was 4.8×10^6U/g DS, there were more negative charges in LB-EPS than in S-EPS and TB-EPS, and this was possible the cause of the decreased proportions of adsorption water in S-EPS and TB-EPS as well as increased proportion in LB-EPS.

After freezing-thaw conditioning, the negative charge in LB-EPS first rose and then reduced, while that in TB-EPS showed an opposite trend. Moreover, it had a lower zeta potential value (-21.17 mV) of LB-EPS and adsorption water had a higher proportion at freezing time of 5 h. These variations were associated with the destruction of EPS structure and cell wall and the release of organic substances after freezing conditioning, which led to the more negatively charged and hydrophilic functional groups in LB-EPS.

3.3 Effect of sludge floc structural properties on the water distribution

EPS extensively existed inside and on the surface of sludge flocs, and a huge network structure was formed between cells and EPS, which could protect sludge from dewatering (Sakohara et al., 2007; Masihi and Gholikandi, 2018). Therefore, EPS could affect the sludge water distribution by affecting the sludge network structure (Sakohara et al.2007).

3.3.1 The change of sludge network structure

3.3.1.1 Steady shear flow

According to Fig. 3, sludge shear stress slowly went up as shear rate increased, while the viscosity was reduced and then tended to be stable. The cause of this variation trend was that the molecular chains inside the sludge system were arranged along the flow field direction, and the destruction rate of physical crosslinking points was greater than the reconstruction rate, so the sludge viscosity began to decline (Wang et al., 2017). These changes suggesting the sludge before and after conditioning possessed the thixotropy or shear thinning characteristics. In addition, the shear stress and viscosity of the raw sludge

were the highest; besides, sludge viscosity gradually descended with EPS extraction. By contrast, it was discovered the viscosity and shear stress of sludge after TB-EPS were increased after LZM conditioning. This was mainly because the organic substances inside the cells were released after LZM conditioning, leading to the increase of sludge viscosity. After freezing conditioning, the changes of sludge viscosity and shear stress were similar to those after LZM conditioning.

To further analysis the rheological behaviors of sludge, the Herschel-Bulkley model was utilized for fitting analysis on the association of shear stress with non-Newtonian fluid shear rate.

$$\tau=\tau_0+K\dot{\gamma}^n$$

Where τ_y was the yield stress, k was used to characterize the fluid viscosity, and n was used to characterize the trend of fluid shear thinning. The greater k value indicated the more viscous fluid. And the smaller n value signified the greater trend of fluid shear thinning and pseudoplastic degree (Farno et al., 2016).

In Table S2, τ_y, k and n values of raw sludge were 1.23 Pa, 1.49 Pa·s^n and 1.30, respectively. With the extraction of EPS, τ_y and n showed a decreasing tendency, signifying the reduction of the critical shear stress value of sludge to flow and the increase of pseudoplastic degree. Compared with the raw sludge, τ_y of the LZM-conditioned sludge was reduced to 0.23 Pa. Moreover, with EPS extraction, τ_y value first decreased and then increased, and the k value also reduced from 4.23 Pa·s^n to 0.006 Pa·s^n and then slightly rose up. This phenomenon was consistent with the change of sludge viscosity after LZM conditioning. After freezing-thaw conditioning, τ_y and k of the sludge were lower than those of the raw sludge, which was similar to the variation of shear stress and viscosity.

3.3.1.2 Dynamic rheological characteristics

There was a binding force network among the bacterial clusters, which became the first network structure, its acting force was weak and first ruptured in the presence of sludge deformation. The second macromolecular long chain with better ductility was more resistant to external deformation (Eshtiaghi et al., 2013; Wang et al., 2017). EPS was a kind of macromolecular polymer, which was capable of inducing mechanical effect through the entanglement of molecular chains (Liu et al., 2013; Chen et al., 2016). Therefore, to further illustrate the effect of EPS on sludge network structure, the sludge rheological property before and after EPS extraction was investigated.

In Fig. 4a, the storage modulus (G') of sludge was greater than the loss modulus (G") within the LVE, which manifested the gel-like structural features and possessed high elasticity (Eshtiaghi et al., 2013). With the extraction of EPS, G' and G" were gradually declined, suggesting the weakness of sludge's elastic property. Compared with the raw sludge, G' and G" of LZM-conditioned sludge were decreased, while G' and G" were increased after TB-EPS extraction. Clearly, LZM attacked and destroyed microbial cell wall, and organic substances were produced in great quantities. Furthermore, the intracellular organic

substances could increase the interaction between sludge flocs and enhance the corresponding sludge network cohesive energy, thus increasing the sludge elastic property after TB-EPS extraction. After freezing conditioning, the elastic characteristic of sludge was weakened and tended to become the flow state after S-EPS and LB-EPS extraction. Moreover, G' and G" were increased after TB-EPS extraction, which was mainly related to the release of organic substances from the microbial cells.

As shown in Fig. S3, G' and G" were not changed significantly, signifying the stable rheological property of sludge with the increase of frequency and time. After LZM or freezing conditioning, both G' and G" were decreased, which was consistent with the results shown in Fig. 4.

3.3.2 The change of sludge particle size

The particle size of raw sludge was 48.1 μm in Fig. 5, and it was not markedly changed after LZM conditioning. Besides, it gradually decreased following S-EPS and LB-EPS extraction, mainly because the sludge microbial cell wall was destroyed after LZM conditioning, causing the destruction of sludge network structure and the reduction of particle size. Additionally, small particles were featured with enlarged specific surface area, which could more easily adsorb water molecules, thus resulting in the increased proportion of capillary water, adsorption water and bound water within sludge flocs (Cai, et al., 2017; Carrasco and Gao, 2019). Compared with the above, after TB-EPS extraction, the sludge particle size significantly increased, with the maximum of 95.72 μm. The reason lied in the released PN containing amino groups with positive charge, which could neutralize the negative charge of sludge surface and promote sludge particle flocculation (Lin, et al., 2020).

Fig. 5 showed that sludge particle size went up after freezing conditioning, with the maximum reaching 181.01 μm, which was mainly caused by the gradual aggregation of the sludge particles gradually aggregated due to the squeezing of ice crystals, thus rendering the increase of particle size. What's more, after S-EPS, LB-EPS and TB-EPS, the sludge particle size showed a similar variation trend to that after LZM conditioning.

3.3.3 The change of sludge fractal dimension

It was illustrated from Fig. 6a, the one-dimensional fractal dimension (D1) value of the raw sludge was 1.19, which was not markedly changed after LZM conditioning. However, D1 increased to 1.27 after LB-EPS extraction. This may be because some inorganic particles were exposed after LB-EPS extraction, resulting in a coarse surface of sludge flocs (Chakraborti et al., 2003). In addition to that, the two-dimensional fractal dimension (D2) displayed an increasing trend in Fig. 6b, indicating the more compact sludge floc structure after EPS extraction. Additionally, D1 showed a decreasing tendency, while D2 was featured with an opposite trend in Fig. 6c-d, which indicated the sludge floc structure became more compact and smoother after freezing-thaw conditioning.

3.4 Effect of EPS on sludge dewaterability

After LB-EPS and TB-EPS extraction, CST was 271 s and 159 s in Fig. S4, maybe because the proportion of bound water, adsorption water and capillary water, in sludge flocs increased after TB-EPS and LB-EPS extraction. As LZM dosage increased, CST gradually decreased after S-EPS and LB-EPS extraction, which showed an increasing trend following TB-EPS extraction, with a maximum value of 332.3 s. This phenomenon was mostly because that LZM conditioning destroyed EPS structure and microbial cell wall and organic substances were released, which could increase the viscosity on sludge particle surface and give rise to the increase of capillary water and absorbed water. After freezing-thaw conditioning, CST was gradually decreased from 61.24 s to 13.1 s, while an increasing trend appeared after TB-EPS extraction, suggesting the difficulty of water migration and transformation, which might be related to the increase of capillary water and adsorption water after TB-EPS extraction.

Conclusion

The proportion of capillary water and adsorption water carried in S-EPS was 59.17% and 40.83%, and that in TB-EPS was 54.77% and 45.23%, respectively. Different from the above, capillary water was accounted for as high as 99.99% in LB-EPS. Capillary water proportion in LB-EPS was decreased after conditioning, while that of adsorption water was increased. It could be attributed to the reduction of EPS viscosity, accompanied by the transformation of negatively charged hydrophilic functional groups from the cells and EPS to the liquid phase. Additionally, EPS could change the sludge floc network structure to affect the distribution of water in sludge. Besides, the Herschel-Bulkley model was utilized for fitting analysis on the association of shear stress with non-Newtonian fluid shear rate. The results indicated τ_y, k and n of raw sludge were 1.23 Pa, 1.49 $Pa \cdot s^n$ and 1.30, respectively. With the extraction of EPS, τ_y value first reduced and then increased, and k also decreased from 4.23 $Pa \cdot s^n$ to 0.006 $Pa \cdot s^n$ and then slightly increased after LZM conditioning. Moreover, the sludge viscosity, shear stress, G', and G" were increased after TB-EPS extraction, indicating the enhancement of sludge network cohesive energy. This observation could promote the sludge to adsorb water molecules, leading to the increase of capillary water, adsorption water and bound water in sludge floc structure, which was also the reason of the the increase of CST after TB-EPS extraction.

Declarations

Ethics approval and consent to participate

Not applicable

Consent for publication

Not applicable

Availability of data and materials

All data generated or analysed during this study are included in this published article [and its supplementary information files].

Competing interests

The authors declare that they have no competing interests.

Funding

This study was supported by the Science and Technology Planning Project of Guangdong Province, China (2016A020221011).

Authors' contributions

All authors contributed to the study conception and design. Material preparation, data collection and analysis were performed by [Feng Lin] and [Bingyun Li]. The first draft of the manuscript was written by [Feng Lin] and all authors commented on previous versions of the manuscript. All authors read and approved the final manuscript.

References

Bradford, M.M.. 1976. A rapid and sensitive method for the quantitation of microgram quantities of protein utilizing the principle of protein-dye binding [J]. Analytical Biochemistry, 72, 248-254.

Cai, C., Liu, H., Wang, M.. 2017. Characterization of antibiotic mycelial residue (AMR) dewatering performance with microwave treatment [J]. Chemosphere, 174, 20-27.

Carrasco, M., Gao, W.. 2019. Sludge particle size and correlation with soluble organic matter and conditioning characteristics after freezing treatments [J]. Water Air and Soil Pollution, 230, 1-9.

Chakraborti, R.K., Gardner, K.H., Atkinson, J.F. Benschoten, J. E.. 2003. Changes in fractal dimension during aggregation [J]. Water Research, 37, 873-883.

Chen, Z., Zhang, W., D Wang, Ma, T., Bai, R., Yu, D.. 2016. Enhancement of waste activated sludge dewaterability using calcium peroxide pre-oxidation and chemical re-flocculation. Water Research, 103, 170-181.

Eshtiaghi, N., Markis, F., Yap, S. D., Baudez, J. C., Slatter, P.. 2013. Rheological characterization of municipal sludge: a review [J]. Water Research. 475, 493-5510.

Farno, E., Baudez, J. C., Parthasarathy, R., Eshtiaghi, N.. 2016. The viscoelastic characterization of thermally-treated waste activated sludge [J]. Chemical Engineering Journal, 304, 362-368.

Guo, X., Liu, J., Xiao, B.. 2014. Evaluation of the damage of cell wall and cell membrane for various extracellular polymeric substance extractions of activated sludge [J]. Journal of Biotechnology, 188, 130-

135.

He, D. Q., Wang, L. F., Jiang, H., Yu, H. Q.. 2015. A Fenton-Like Process for the Enhanced Activated Sludge Dewatering [J]. Chemical Engineering Journal, 272, 128-134.

Li, Y., Yuan, X., Wu, Z., Wang, H., Xiao, Z., Wu, Y., Chen, X., Zeng, G.. 2016. Enhancing the Sludge Dewaterability by Electrolysis/Electrocoagulation Combined with Zero-Valent Iron Activated Persulfate Process [J]. Chemical Engineering Journal, 303, 636-645.

Lin, F., Li, J. G., Chai, X. S., Zhang, Z. B., Liu, M.. 2020, Determination of Water Distribution in Sludge by A Multiple Headspace Extraction Analytical Technique [J]. Journal of Chromatography A, 1628, 461449.

Lin, F., Li, J., Liu, M., Yu, P., Zhu, X.. 2020. New insights into the effect of extracellular polymeric substance on the sludge dewaterability based on interaction energy and viscoelastic acoustic response analysis [J]. Chemosphere, 261, 127929.

Lin, F., Zhu, X., Li, J., Yu, P., Luo, Y., Liu, M.. 2019. Effect of extracellular polymeric substances (EPS) conditioned by combined lysozyme and cationic polyacrylamide on the dewatering performance of activated sludge [J]. Chemosphere, 235, 679-689.

Liu H., Yang J., Zhu N., Zhang H., Li Y., He S., Yang C., Yao H.. 2013. A comprehensive insight into the combined effects of Fenton's reagent and skeleton builders on sludge deep dewatering performance [J]. Journal of Hazardous Materials, 258-259, 144-150.

Liu, J., Yu, D., Zhang, J., Yang, M., Wang, Y., Wei, Y. Tong, J.. 2016. Rheological properties of sewage sludge during enhanced anaerobic digestion with microwave-H_2O_2 pretreatment [J].Water Research 98, 98-108.

Mahmoud, A., Olivier, J., Vaxelaire, J., Hoadley, A.. 2011. Electro-dewatering of wastewater sludge: Influence of the operating conditions and their interactions effects [J].Water research, 45, 2795-2810.

Masihi H., Gholikandi G. B.. 2018. Employing Electrochemical-Fenton process for conditioning and dewatering of anaerobically digested sludge: A novel approach [J]. Water Research, 144, 373-382.

Niu, M., Zhang, W., Wang D., Chen, Y., Chen, R.. 2013. Correlation of physicochemical properties and sludge dewaterability under chemical conditioning using inorganic coagulants. Bioresource Technology, 144, 337-343.

Poxon T. L., Darby J. L.. 1997. Extracellular polyanions in digested sludge: Measurement and relationship to sludge dewaterability [J]. Water Research, 31, 749-758

Raunkjær, K., Hvitved-Jacobsen, T., Nielsen, P. H.. 1994. Measurement of pools of protein, carbohydrate and lipid in domestic wastewater [J]. Water Research, 28, 251-262.

Sakohara, S., Ochiai E., Kusaka T.. 2007. Dewatering of activated sludge by thermosensitive polymers [J]. Separation and Purification Technology, 56, 296-302.

Suzuki M., Tsuge S., Takeuchi T.. 1970. Gas chromatographic estimation of occluded solvents in adhesive tape by periodic introduction method [J]. Analytical Chemistry, 42, 1705-1708.

Vaxelaire, J., Cezac, P., 2004. Moisture distribution in activated sludges: a review. Water Research. 38 (9), 2215-2230.

Wang, B. B., Liu, X. T., Chen, J. M., Peng, D. C., He, F.. 2017. Composition and functional group characterization of extracellular polymeric substances (EPS) in activated sludge: the impacts of polymerization degree of proteinaceous substrates [J]. Water Research, 129, 133-142.

Wang, H. F., Ma, Y. J., Wang, H. J., Hu, H., Zeng, R. J.. 2017. Applying rheological analysis to better understand the mechanism of acid conditioning on activated sludge dewatering [J]. Water Research, 122, 398-406.

Wang L., Li A., Chang Y.. 2017. Relationship between enhanced dewaterability and structural properties of hydrothermal sludge after hydrothermal treatment of excess sludge [J]. Water Research, 112, 72-82.

Wu, B., Zhou, M., Dai, X.H., Chai, X.. 2018. Mechanism insights into bio-floc bound water transformation based on synchrotron X-ray computed microtomography and viscoelastic acoustic response analysis [J]. Water Research, 142, 480-489.

Xiao J., Ge D.D., Yuan H. P., Zhu N. W.. 2020. Waste activated sludge conditioning in a new Fe^{2+}/persulfate/tannic acid process: Effectiveness and optimization study to enhance dewaterability [J]. Journal of Environmental Chemical Engineering, 8, 103785.

Xiao, K., Chen, Y., Jiang, X., Tyagi, V. K., Zhou, Y.. 2016. Characterization of key organic compounds affecting sludge dewaterability during ultrasonication and acidification treatments [J]. Water Research, 105, 470-478.

You, G., Wang, P., Hou, J., Wang, C., Xu, Y., Miao, L., Lv B.,Yang, Y.Liu, Z. Zhang, F.. 2017. Insights into the short-term effects of CeO_2 nanoparticles on sludge dewatering and related mechanism [J].Water Research, 118, 93-103.

Zhang S. X., Chai X. S., He L.. 2016. Accurate determination of fiber waterretaining capability at process conditions by headspace gas chromatography [J]. Journal of Chromatography A, 1464: 50-54.

Zhang, W., Dong, B. Dai, X.. 2019. Mechanism analysis to improve sludge dewaterability during anaerobic digestion based on moisture distribution [J]. Chemosphere, 227, 247-255.

Figures

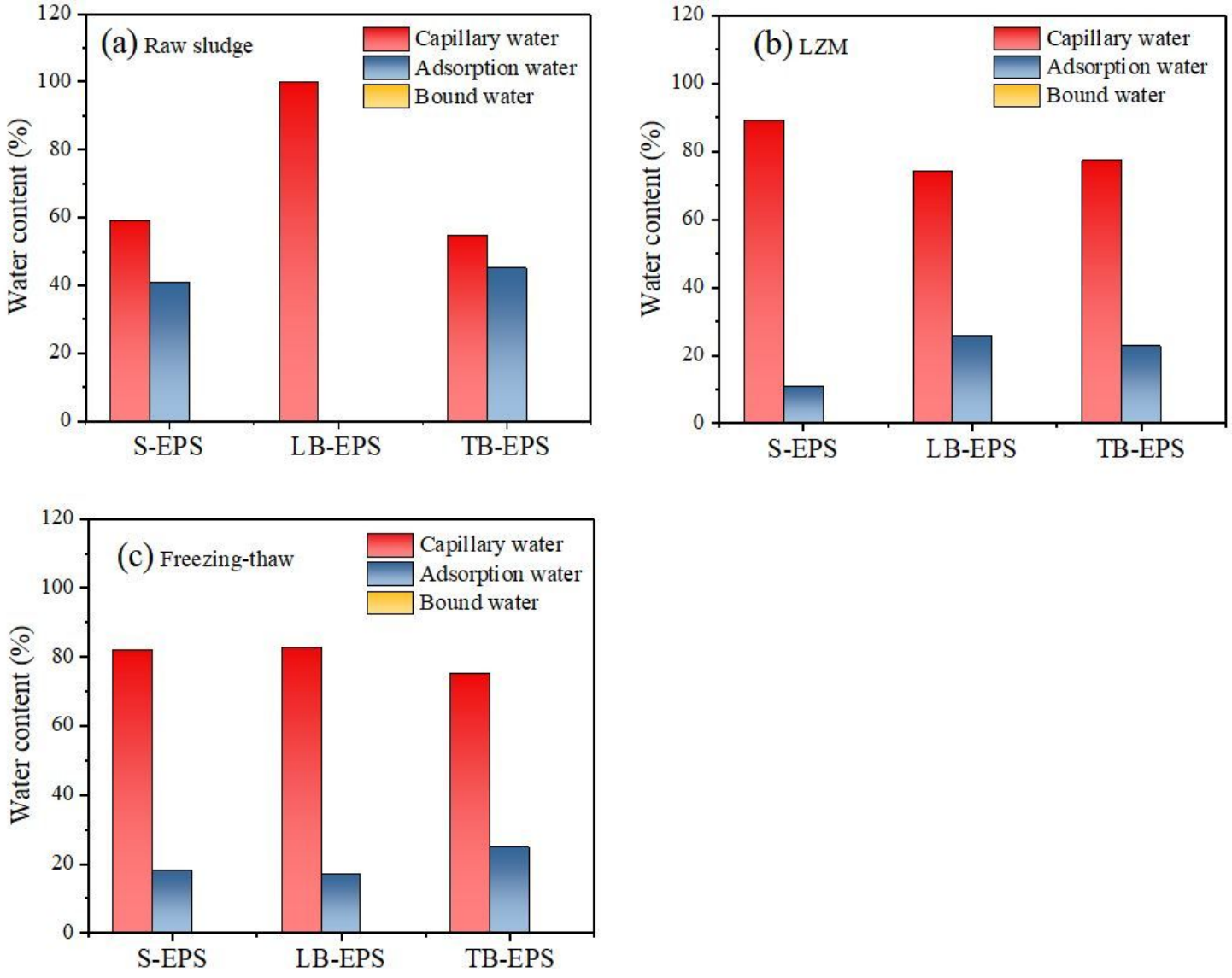

Figure 1

The proportion of water in EPS (a) Raw sludge; (b) LZM; (c) Freezing-thaw

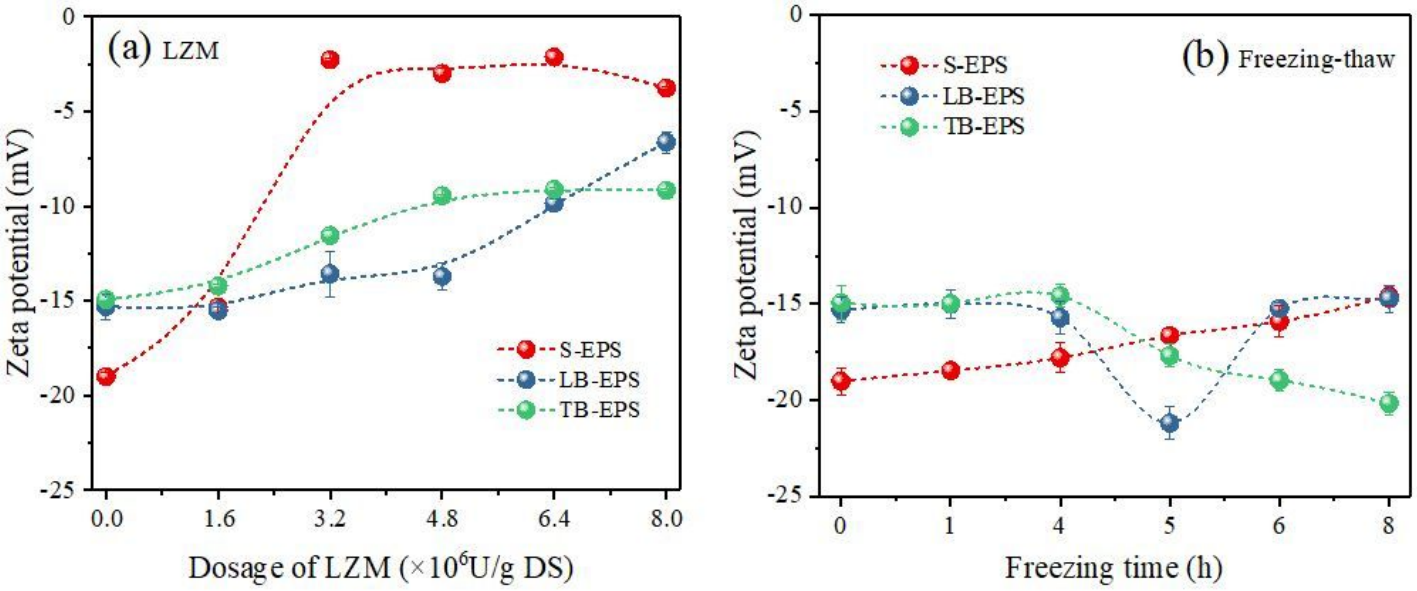

Figure 2

Zeta potential of EPS (a) LZM; (b) Freezing-thaw

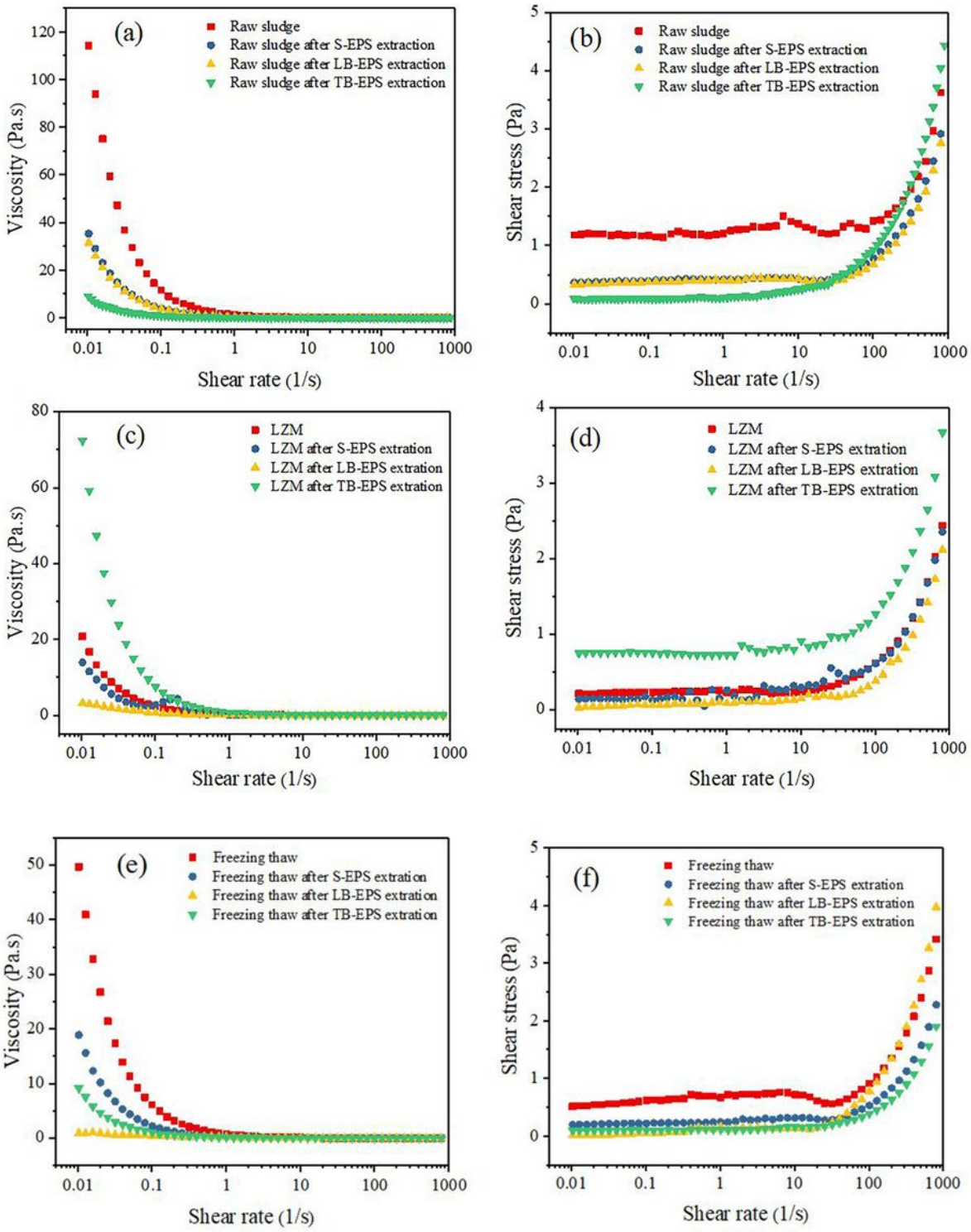

Figure 3

Viscoelastic properties of sludge flocs (a-b) Raw sludge; (c-d) LZM; (e-f) Freezing-thaw

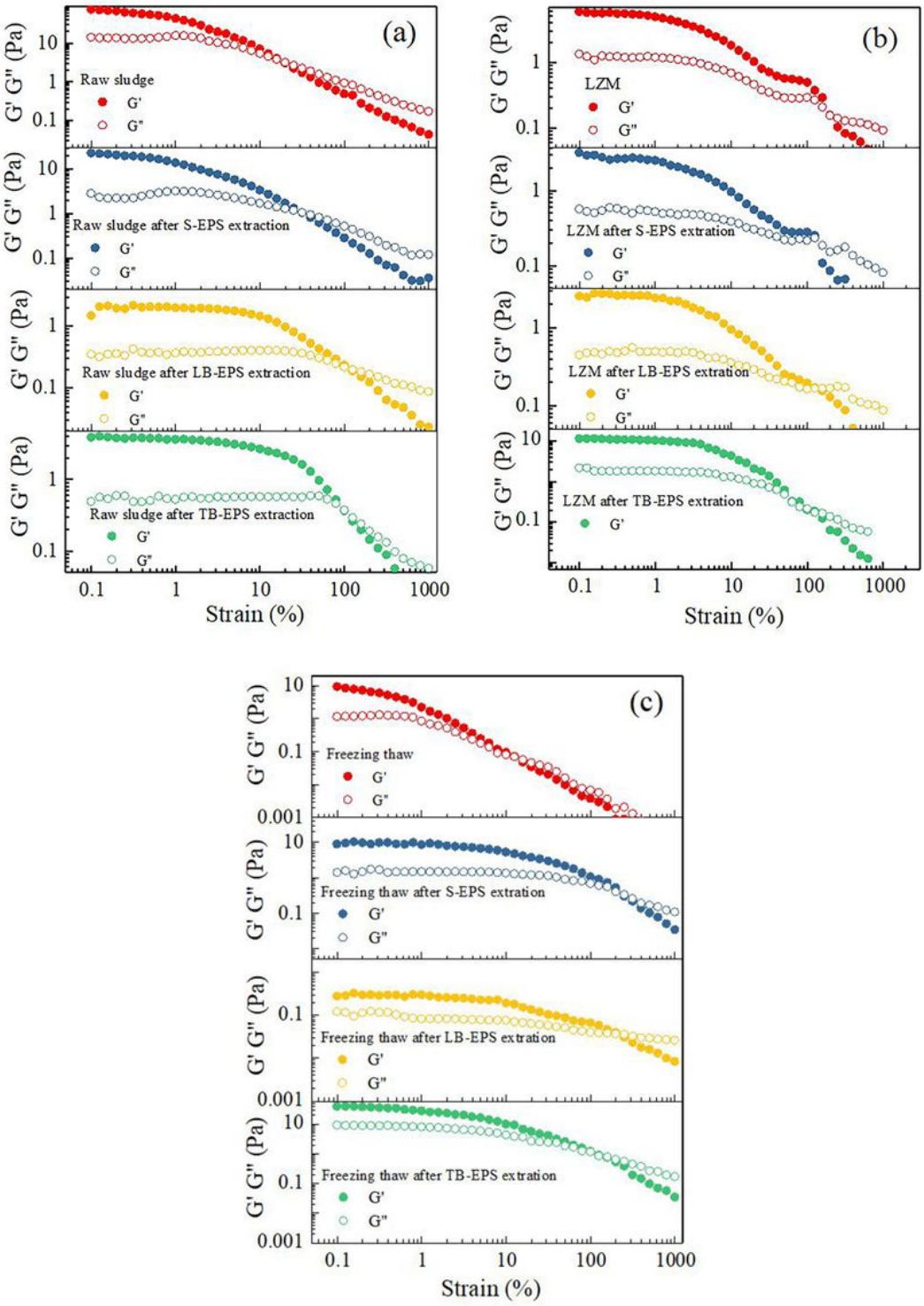

Figure 4

Dynamic strain sweep curve (a) Raw sludge; (b) LZM; (c) Freezing-thaw

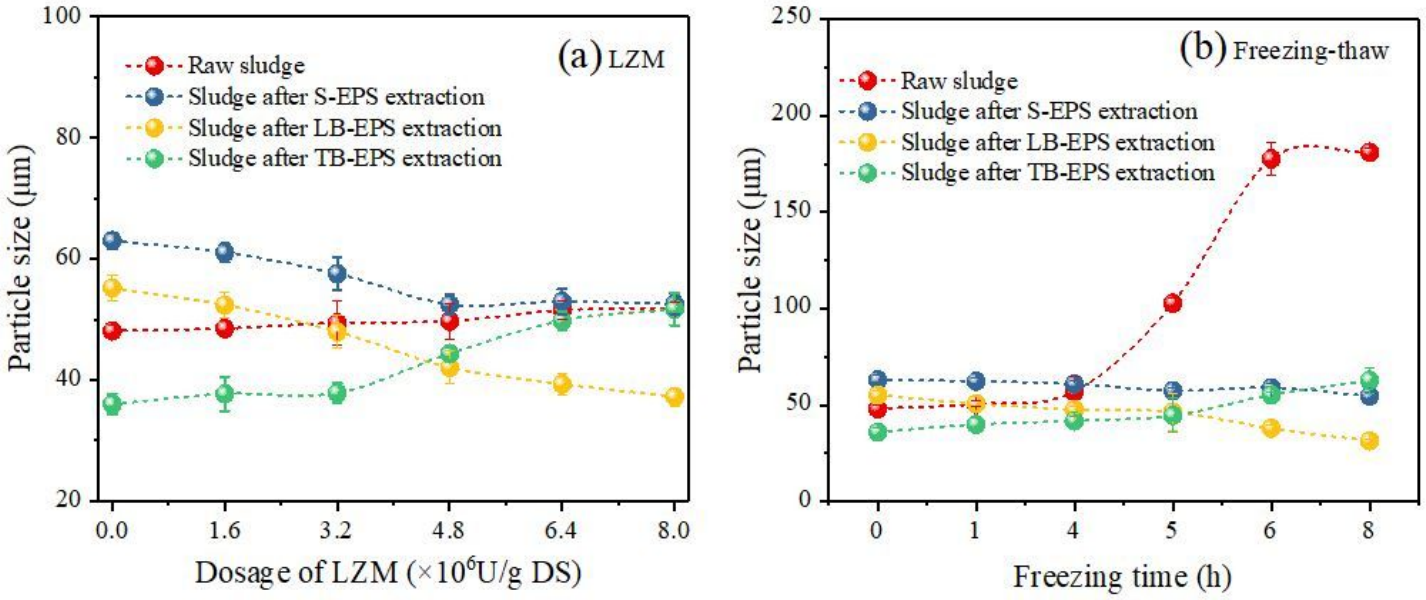

Figure 5

Sludge particle size (a) LZM; (b) Freezing-thaw

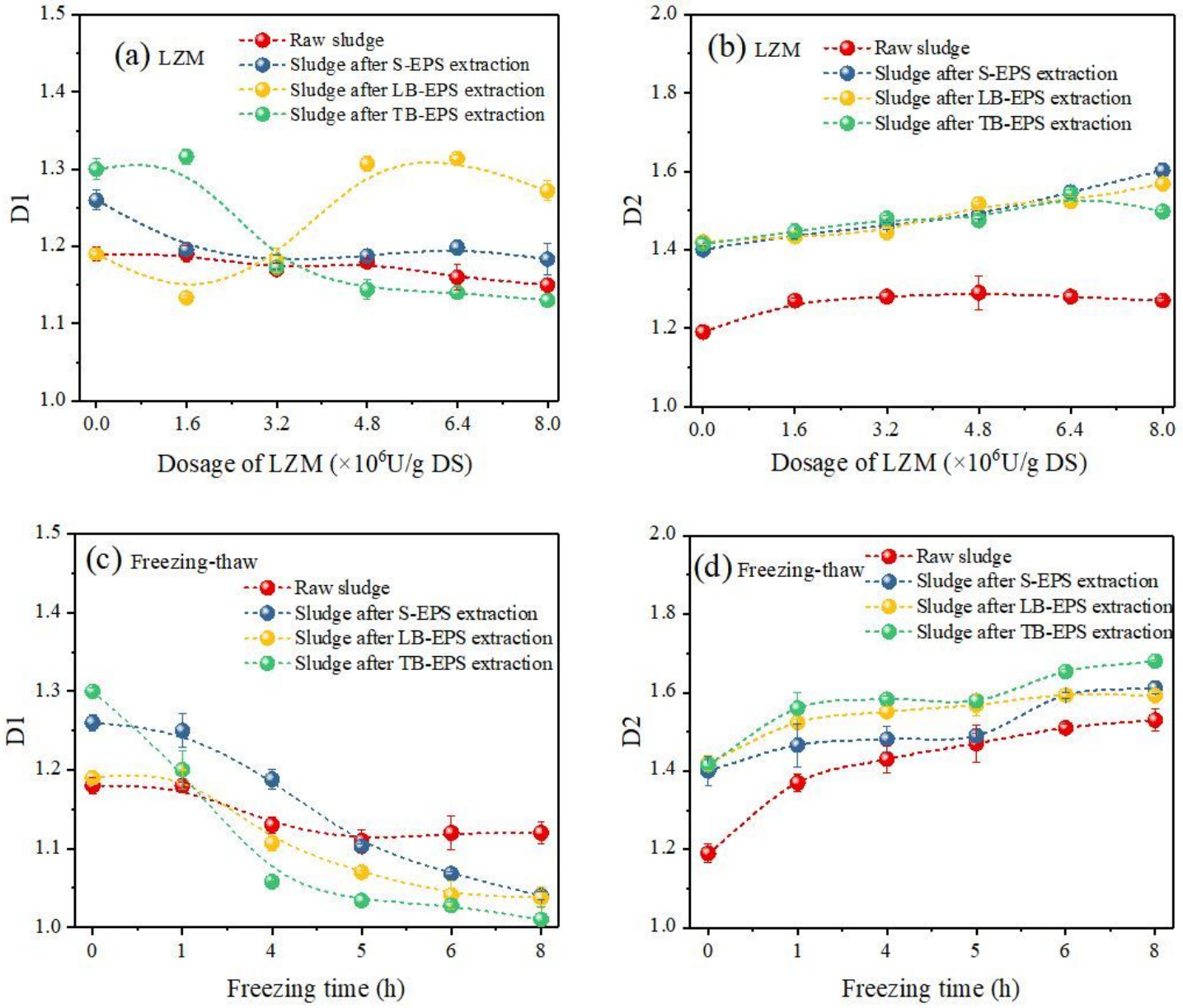

Figure 6

Sludge fractal dimension (a-b) LZM; (c-d) Freezing-thaw

Supplementary Files

This is a list of supplementary files associated with this preprint. Click to download.

- SupplementaryMaterials.doc